The Optimization for Hyperbolic Positioning of UHF Passive RFID Tags

Haishu Ma, Yi Wang, Kesheng Wang, and Zongzheng Ma

***Abstract*— This paper presents a fine-grained positioning method for radio frequency identification (RFID). The proposed method applies hyperbolic positioning to locate ultrahigh frequency passive RFID tags. In our design, finding the tagged object's location is formulated as an optimization problem. Phase values, collected by the moving antenna, are exploited to achieve the optimal solution. The intuition of hyperbolic positioning lies in that the difference of distances from a target tag to two antennas can be inferred from phases. When integrating hyperbola curves together, optimization method can be performed to achieve the object's location. Particle swarm optimization is then applied to enhance computational ability. For random phases, polynomial regression is employed to model the relationship between phase values and distances. We implement a prototype of hyperbolic positioning optimization to pinpoint the RFID tag's location and evaluate its performance in our laboratory environment. Compared with other RFID localization methods, i.e., received signal strength indicator based and phase-based approaches, our design shows greater tolerance to tag diversity and tag orientation.**

***Note to Practitioners*—Radio frequency identification (RFID), as a crucial component of the Internet of things, has been widely deployed in many industrial applications ranging from logistics to retail. There are increasing needs for RFID to not only detect whether the tagged object is within the radio range, but also locate the object with high accuracy. Current RFID systems addressing these problems are either expensive or complex to implement. The RFID-based localization method presented in this paper is cost-efficient and computationally inexpensive. We consider using commercial off-the-shelf RFID devices without deployment of the reference tags to locate the target object. The antenna is mounted on a mobile vehicle to emulate the antenna array. Due to the fact that the target tag lies on the hyperbolic curve with two antennas' positions as the foci, this paper suggests constructing multiple hyperbolas to determine the target position based on the virtual antenna array. The experimental results demonstrate that the proposed approach is feasible and achieves a median accuracy of 12 cm.**

***Index Terms*— Hyperbolic positioning, indoor localization, optimization, radio frequency identification (RFID).**

Manuscript received May 9, 2016; revised September 12, 2016 and December 16, 2016; accepted January 18, 2017. Date of publication February 20, 2017; date of current version October 4, 2017. This paper was recommended for publication by Associate Editor J. Mitsugi and Editor L. Shi upon evaluation of the reviewers' comments.

H. Ma and K. Wang are with the Knowledge Discovery Laboratory, Norwegian University of Science and Technology, N-749 Trondheim, Norway (e-mail: haishu.ma@ntnu.no; kesheng.wang@ntnu.no).

Y. Wang is with the School of Materials, University of Manchester, Manchester M13 9PL, U.K. (e-mail: yi.wang-2@manchester.ac.uk).

Z. Ma is with the Mechanical Engineering Department, Henan Institute of Engineering, Zhengzhou 451191, China (e-mail: zongzhengma@gmail.com).

Color versions of one or more of the figures in this paper are available online at http://ieeexplore.ieee.org.

Digital Object Identifier 10.1109/TASE.2017.2656947

I. Introduction

RADIO frequency identification (RFID) has been widely adopted in supply chain management and warehousing for the purpose of automatic identification and tracking of objects. A typical RFID system is made of tags, reader, and antenna. RFID reader can communicate with the tag in an electromagnetic field. Whenever a tag enters the interrogation region, it can be detected by the RFID reader [1]. Depending on the power output of reader and the types of tag, the read range of RFID system can be as far as tens of meters [2]. Under many circumstances, it is not enough to only identify whether the RFID-tagged object is within the read range. For example, a robot arm can reach for a target object, pick it up, and deliver it from assembly lines, which require locating the object to the accuracy of the mm-level [3]. Hospitals and health centers will greatly benefit from knowing the exact location of misplaced medical equipment [4], [5]. The working efficiency of hospital staff will be improved and the patients' safety will be increased. More than 90% of baggage losses usually occur when there are tracking and sorting errors in airport conveyors. An RFID-assisted sortation system has been deployed in airports to track baggage with high precision [6].

Fine-grained RFID positioning approaches have been studied for decades [6], [7], [19], [32]. These works can mainly be divided into two categories, received signal strength indicator (RSSI)-based methods and phase-based methods. Early RFID localization methods focused on RSSI [7]–[10]. RSSI has a direct relationship with distance and the RSSI-based system is not difficult to implement. The accuracy of RSSI varies widely due to the tags' orientation and antenna gain [11], [13], which make RSSI not a reliable indicator for positioning. Growing attention has been drawn to phase-based localization methods [13]–[25], which can be classified into two groups further, i.e., angle of arrival (AOA) and synthetic aperture radar (SAR). AOA-based methods usually deploy multiple antennas to receive the phase value [13]–[18], which is expensive to implement. Moreover, it remains a great challenge to limit the antennas' spacing to less than half the wavelength for AOA methods. This constraint is difficult to meet, especially for directional antennas, which are usually too large. Different from AOA methods, many SAR methods measure phase values by employing a moving antenna to emulate the antenna array [19]–[22], which is also adopted in our design. Additionally, many existing RFID localization methods [7], [19], [23]–[25], including phase based and RSSI based, rely on deploying dense reference RFID tags at known

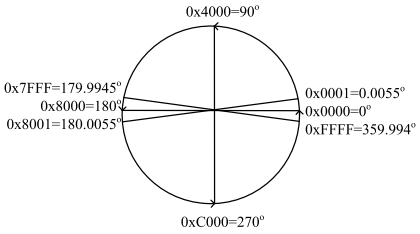

Fig. 1. Mapping of phase to the 16-bit reported value.

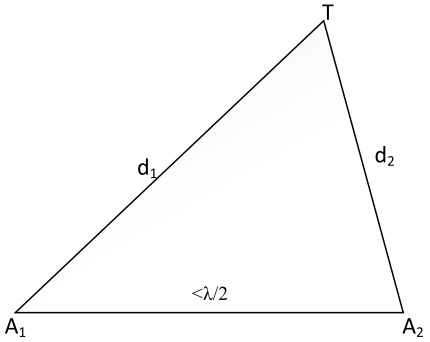

Fig. 2. Triangle constraint. When the distance between two antennas is less than half the wavelength, the phase difference between two consecutive measurements can be confined within 2π.

positions to estimate the target object. The accuracy of these methods largely depends on the density of reference tags.

This paper proposes hyperbolic positioning optimization, a fine-grained localization method, which leverages the phase value received from reader to locate target object attached with RFID tag without need of reference tags. Most [commercial off-the-shelf (COTS)] RFID devices support phase report feature. The reader employed in our design is Sirit Infinity 610. The phase estimate is reported as a hexadecimal number scaled from 0 to 2π and the resolution is about 0.005°, as shown in Fig. 1.

Although the phase accuracy has the potential to locate the object within mm-level, there are innate challenges for phase value. First, the phase value has ambiguity and repeats every 2π radians. Therefore, phase value cannot reflect the distance directly. Second, different antennas and tags will introduce extra phase shifts to the measured total phase. The device diversity is a constant parameter but calibration of all RFID tags and readers is impractical and time-consuming. In order to deal with the above challenges, we propose the hyperbolic positioning optimization method using COTS RFID devices. Phase ambiguity can be solved by phase difference between two different antennas when the space of the two antennas is less than half the wavelength [20]. Actually, this is a simple triangle inequality, as illustrated in Fig. 2.

According to the triangle constraint, the distance difference will be less than half the wavelength and the phase difference will be less than 2π. Because hyperbola is the locus of points where the distance difference to the two foci is a constant, a hyperbola can be constructed once the distance difference is known. Here, the two antennas' locations are the foci, and the position of the target tag lies on the hyperbola curve. When multiple hyperbolas are built, their common intersection will be the object's position in theory. This hyperbolic positioning method is inspired by Liu *et al*. [32], but we extended its research in terms of hyperbolic curve construction. One way to build many hyperbola curves is to deploy antenna array, which is adopted in [15] and [26]. However, antenna array is not cost-effective and another disadvantage of it is that the device diversity cannot be eliminated. Our design simulates the antenna array through antenna motion along a straight line at a constant velocity. This method should attribute to SAR, which was first used in the radar system for terrain imaging [19]. Different from the physical antenna array, this virtual antenna array is actually the same antenna and therefore, there is no antenna diversity. The elimination of tag diversity will be elaborated in Section IV. Hyperbolic positioning optimization will combine multiple hyperbolas together to achieve the optimal solution. Usually, finding the optimum is computationally expensive. Our design will introduce the computational intelligence method for solving the optimization problem. In addition, we also propose the regression analysis to address the random phase problem. In sum, this paper made the following contributions.

First, the hyperbolic positioning optimization method makes the RFID localization system cost efficient and easy to implement because only COTS are used and there is no need to deploy reference tags. Moreover, antenna array can be emulated by antenna motion, which reduces the cost further.

Second, our design effectively limits the negative impacts of phase noise using regression analysis.

Third, to the best of our knowledge, we are the first to introduce particle swarm optimization (PSO) into phase-based RFID indoor positioning, which makes the computation greatly enhanced.

The rest of this paper is organized as follows. The background and empirical studies are introduced in Section II. We present the general overview of hyperbolic positioning optimization method in Section III and the technical details are elaborated in Section IV. The implementation of our design is described in Section V and evaluated in Section VI. Finally, Section VII concludes our work.

II. Background

Ultrahigh frequency (UHF) RFID system communicates through backscatter radio link. Fig. 3 displays the backscatter communication between a reader and a tag. The passive RFID tag has no battery; instead, they draw power from the reader, which transmits electromagnetic waves that induce a current in the tag's antenna. The RF signal transmitted by the reader is reflected off the tag, received back at the reader, and processed to decode the data. The tag will reply the reader's query by changing the impedance on its antenna and modulates its data on the backscatter signals using ON_OFF keying [6].

A. RF Phase

Most COTS RFID reader can report phase value θ, which is the phase shift between the transmitted and the received signal. Whenever a tag is interrogated by a reader, phase report is generated. As illustrated in Fig. 3, d is the distance from tag to reader. The total propagation distance of RF signal

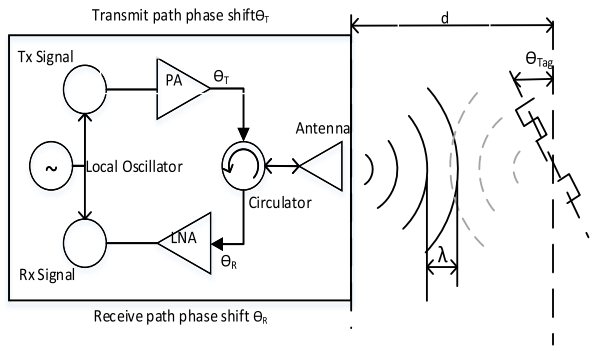

Fig. 3. Radio wave propagation between reader and tag (adapted from [6]).

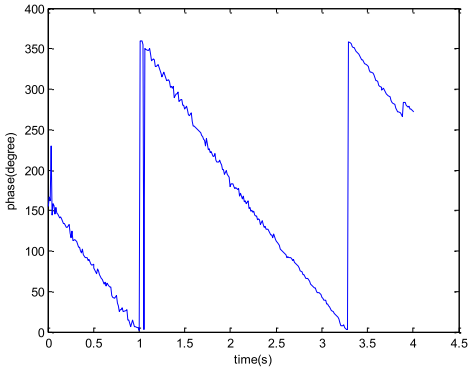

Fig. 4. Phase ambiguity. The measured phase will repeat every 360°.

from the reader to the tag and back again is $2d$. However, reader's transmitter, receiver circuits, and tag's antenna will all contribute extra phase rotations, which make the measured phase not purely related with distance between the reader and tag. The measured phase [27] is a function of the wavelength λ and the total propagation distance $2d$. The formula can be expressed as

$$\theta = \left(\frac{2\pi}{\lambda} \times 2d + \theta_T + \theta_R + \theta_{Tag}\right) \bmod 2\pi \qquad (1)$$

where θ_T, θ_R, and θ_{Tag} are the additional phase rotations introduced by reader transmitter, receiver, and tag, respectively. They are what we call device diversity. The equation notation in (1) is inspired by Yang *et al.* [6]. How to derive the distance from the phase and get rid of the device diversity remains a challenge for RFID positioning using phase measurement. Sirit Infinity 610, the reader that we used in our design, supports phase resolution with 0.005°. Theoretically, the positioning resolution based on the measured phase value can achieve an accuracy of $320 \times 0.005/360 = 0.004$ mm.

B. Phase Ambiguity

We place a tag on the moving conveyor, which will take the tag toward antenna at a constant velocity. When the tag is interrogated by reader, the timestamp will be reported. Then, we can leverage the timestamp to plot the phase change along with the time lapse. Fig. 4 shows that phase will repeat about every 2.26 s. The velocity of conveyor is known in advance, which is 75 mm/s. Based on conveyor velocity, we find that when the distance between antenna and tag

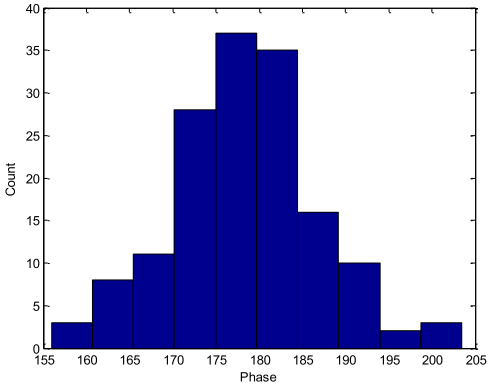

Fig. 5. Random phase. The measured phase is different every time it is interrogated by the reader.

reduces by nearly 17 cm, the phase will repeat 360°. The signal's wavelength can be calculated as $\lambda = c/f$, where c is denoted as the speed of light. For an RF carrier frequency of 865 MHz, the wavelength is 34 cm. Hence, the distance reduction from the antenna to the tag is half the wavelength. This is consistent with theory and phase value is demonstrated to be indeed a reliable indicator for positioning. Nevertheless, phase ambiguity is a challenge for accurate positioning.

C. Random Phase

One interesting finding is that when we place the same tag at the same position and keep the distance from tag to reader unchanged, the phase measurement is not the same every time. Fig. 5 shows the phase distribution of the same tag, which is interrogated for 153 times. The mean phase value is 178.4523° and the standard deviation is 8.1854°. The underlying tag phase θ is not directly observable but is estimated from the noisy received signal. The quality of this estimate is dependent on the RF noise environment. This means that a complex environment will exert unexpected impact on the phase report, which will lead to measurement error. Correction techniques are needed to remedy this situation.

III. Method Overview

Hyperbolic positioning optimization is a phase-based fine-grained RFID localization approach. Our design greatly reduces the positioning system cost using COTS devices and effectively limits the negative impacts of phase ambiguity and device diversity using hyperbolic positioning, which is attributed to [32]. Moreover, we utilize the antenna motion to construct multiple hyperbolas and introduce regression analysis to tackle the random phase problem. The resolution of our method can achieve centimeter accuracy.

In order to locate the target object attached with UHF RFID tag, hyperbolic positioning optimization needs to proceed with the following steps:

1) virtual antenna array queries the target object to collect the phase values;
2) construction of single hyperbola curve based on the phase report;
3) acquiring multiple of hyperbola curves through antenna motion;

4) performing computational intelligence method on integration of multiple hyperbolas to locate the target.

The technical details of the above steps will be elaborated in the following section. Our method is presented in a 2-D scenario, and the tag and the antenna are placed in the same plane.

IV. Hyperbolic Positioning Optimization

A. Hyperbolic Curve Construction

Hyperbola is defined as the locus of points where the distance difference Δd to the two given fixed points is a constant. Suppose there are two antennas, A1 and A2, querying the target tag T. Let $d(T, A_k)$ be the distance from tag T to antenna A_k. Then, the theoretical phase value θ measured by A1 and A2 can be computed as

$$\theta_1 = 2\pi \frac{2d(T, A_1)}{\lambda} + \theta_{T1} + \theta_{R1} + \theta_{Tag1} + 2k_1\pi \tag{2}$$

$$\theta_2 = 2\pi \frac{2d(T, A_2)}{\lambda} + \theta_{T2} + \theta_{R2} + \theta_{Tag2} + 2k_2\pi. \tag{3}$$

The distance difference Δd can be derived by subtracting the above two equations as

$$\Delta d = |d(T, A_1) - d(T, A_2)| = \frac{\lambda}{4\pi}(\theta_1 - \theta_2 - \delta + 2k\pi) \tag{4}$$

where $\delta = \theta_{T1} - \theta_{T2} + \theta_{R1} - \theta_{R2}$ is a constant term. θ_{Tag1} can be wiped out because A1 and A2 query the same tag. From (4), the distance difference Δd can be inferred from phase difference. As long as the distance difference is known, a hyperbola can be constructed with the antennas' positions as the two foci. The hyperbola equation can be formalized as

$$|d(X, A_1) - d(X, A_2)| = \frac{\lambda}{4\pi}(\theta_1 - \theta_2 - \delta + 2k\pi) \tag{5}$$

where X is a point in the hyperbola curve. Particularly, when the two foci locate in x-axis and the origin of coordinate system is the center of the foci, the above formula can be defined as

$$\frac{x^2}{a^2} - \frac{y^2}{b^2} = 1 \tag{6}$$

where

$$a = \frac{|d(T, A_1) - d(T, A_2)|}{2}, \quad b = \sqrt{c^2 - a^2}, \quad c = \frac{|\text{A1A2}|}{2}.$$

One interesting observation is that the diversity term δ can be eliminated when virtual antenna array is adopted. Since the two antennas are derived from antenna motion, there is actually only one antenna. Equation (5) can be simplified as

$$|d(X, A_1) - d(X, A_2)| = \frac{\lambda}{4\pi}(\theta_1 - \theta_2 + 2k\pi). \tag{7}$$

Especially, when the distance between A_1 and A_2 is less than half the wavelength, the distance difference Δd can be derived using

$$\Delta d = \begin{cases} \dfrac{\lambda(\theta_1 - \theta_2)}{4\pi}, & (\theta_1 - \theta_2) * \Delta d > 0 \\ \dfrac{\lambda(2\pi + \theta_1 - \theta_2)}{4\pi}, & (\theta_1 - \theta_2) < 0 \text{ and } \Delta d > 0 \\ \dfrac{\lambda(\theta_1 - \theta_2 - 2\pi)}{4\pi}, & (\theta_1 - \theta_2) > 0 \text{ and } \Delta d < 0. \end{cases} \tag{8}$$

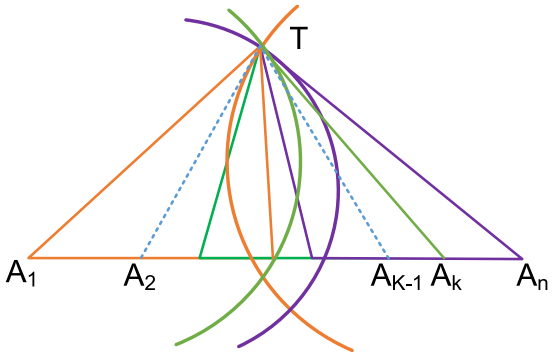

Fig. 6. Hyperbolic positioning. The target position should be the common intersection of multiple hyperbolas.

The above equation can be derived from triangle inequality. The sum of the lengths of any two sides of a triangle must be greater than the third side. When $|A_1A_2|$ is less than half the wavelength, as shown in Fig. 2, the distance difference meets the inequation

$$|d(X, A_1) - d(X, A_2)| < \frac{\lambda}{2}. \tag{9}$$

If $(\theta_1 - \theta_2) * \Delta d > 0$, then from (7), we can obtain the inequation

$$\Delta d = \frac{\lambda}{4\pi}(\theta_1 - \theta_2) + \frac{k\lambda}{2} < \frac{\lambda}{2}. \tag{10}$$

The above inequation can only be true when k equals 0. If $(\theta_1 - \theta_2) < 0$ and $\Delta d > 0$, then only when k equals 1, (10) can be true. In the same way, if $(\theta_1 - \theta_2) > 0$ and $\Delta d < 0$, (10) can be guaranteed to be true only when k equals -1.

Through triangle inequality, phase ambiguity can be dispelled. According to (8), distance difference can be inferred from phase difference. In this way, the hyperbola with the target object constrained on the curve can be constructed. However, even when we restrict the target object on the hyperbola curve, its accurate position is still unknown. One method to pinpoint the target position is to construct multiple hyperbola curves through antenna array.

B. Acquiring Multiple Hyperbola Curves

Fig. 6 shows an antenna array with n antenna components. Antenna array will query the target tag and collect the phase report. Based on the method we described in the above section, multiple hyperbola curves can be constructed. Theoretically, their common intersection will be the position of the target tag. Nevertheless, as we explained previously, deploying antenna array is not cost efficient in practice. Our design aims to use the COTS devices to reduce cost, so we leverage antenna motion to simulate the antenna array. This idea is motivated by Yang *et al.* [6], which views the stationary antenna moves in the opposite direction when the tag is moving along a known trajectory. While in our design, the antenna is really moving along a track.

We emulated the antenna array through moving the antenna at a constant speed along a straight line. The moving antenna will interrogate the target tag at the same time. Suppose the target tag is queried for n times by moving antenna at different

timeslots $(t_0, t_1 \ldots t_{n-1})$, and the velocity of antenna is v. The term t_0 is the time when the target tag is first interrogated by the antenna. The timestamps can be normalized to be the following equation:

$$T = t_0 + (0, \Delta_1, \Delta_2 \ldots \Delta_k \ldots \Delta_{n-1}) \tag{11}$$

where $\Delta_k = t_k - t_0$ denotes the time difference.

At time t_k, the virtual antenna's position can be calculated by the following equation:

$$A_k = A_0 + v \times \Delta_k \tag{12}$$

where A_0 is the initial position of moving antenna.

In theory, as long as the initial position A_0 is known, multiple hyperbola curves can be acquired.

C. Optimization of Multiple Hyperbolas

After acquiring multiple hyperbola curves, the last step is to find the common intersection of the combined hyperbola equations, which is not easy to solve. In our design, locating the target tag can be regarded as an optimization problem. Inspired by PSO's advantages [28], we decided to implement PSO in our design to achieve the optimum solution. PSO is easier to implement with a few parameters to tune and is computationally inexpensive [29]. This is exactly what we need to find the solution of combined hyperbola curves.

In order to implement PSO, we have to define the objective function first. In our design, we want to optimize the combined multiple hyperbola equations. Therefore, the objective function can be determined as

$$J = \sum_{i=0}^{n-1} \left(d(X, A_i) - d(X, A_0) - \frac{\lambda}{4\pi} (\theta_i - \theta_0 + 2k\pi) \right)^2 \tag{13}$$

subject to

$$\Delta d = \begin{cases} \dfrac{\lambda(\theta_i - \theta_0)}{4\pi}, (\theta_i - \theta_0) * \Delta d > 0 \\ \dfrac{\lambda(2\pi + \theta_i - \theta_0)}{4\pi}, (\theta_i - \theta_0) < 0 \text{ and } \Delta d > 0 \\ \dfrac{\lambda(\theta_i - \theta_0 - 2\pi)}{4\pi}, (\theta_i - \theta_0) > 0 \text{ and } \Delta d < 0 \end{cases} \tag{14}$$

where $d(X, A_i)$ denotes the distance from point X to antenna's ith position and θ_i represents the ith phase measured by the moving antenna. Both the phase difference and distance difference is calculated by subtracting the initial phase and antenna position.

J denotes the objective that we want to optimize. Obviously, the point X that makes the J minimum is the target tag location. In theory, the minimum J equals 0. However, because of the complex environment impacts, the minimum J does not absolutely equal 0.

The general steps of PSO are as follows.

1) Initialize parameters, e.g., maximum number of iterations, swarm size, and initial particle velocities $\vec{v}_i$ and positions $\vec{x}_i$.
2) Loop.
3) Evaluate each particle's position $\vec{x}_i$ according to the objective function.

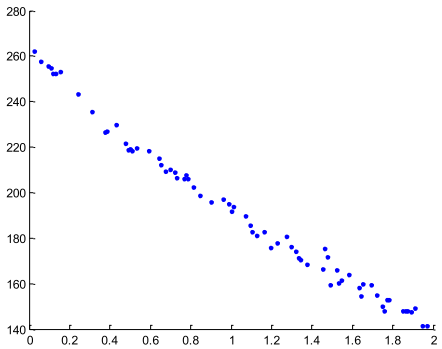

Fig. 7. Measured phase values through antenna motion.

4) Find the best solution of each particle $\vec{p}_i$ so far.
5) Find the best solution of all particles $\vec{p}_g$ until now.
6) Update the velocity of each particle at tth iteration according to

$$\vec{v}_i(t+1) = \omega \cdot \vec{v}_i(t) + c_1 r_1 (\vec{p}_i - \vec{x}_i(t)) + c_2 r_2 (\vec{p}_g - \vec{x}_i(t)) \tag{15}$$

where c_1 and c_2 are acceleration coefficients and r_1 and r_2 are random numbers distribution on [0, 1].

7) Update the position of each particle tth iteration according to the following equation:

$$\vec{x}_i(t+1) = \vec{x}_i(t) + \vec{v}_i(t+1). \tag{16}$$

8) If a criterion is met, exit loop.

Usually, the criterion is set to be the maximum iterations or the number of iterations for which the objective has not changed.

We conducted a pilot experiment to illustrate the mechanism of hyperbolic positioning optimization in detail. In our experiment, the target tag is queried 71 times by the moving antenna. The measured phase through antenna motion is shown in Fig. 7. The ground truth of the target tag's position is (310, 450).

We partitioned the motion reader's interrogation region (1000 mm × 1000 mm) into many grids. Fig. 8 shows the possibility of each grid to be the target position based on (13). Obviously, the pixel with the highest value is the target object position. The pixel (218, 330) has the highest pixel value and the deviation from the ground truth is about 151.21 mm away.

As shown in Fig. 8, there is a strip of pixels whose values are relatively very high, which makes PSO easily trapped into the local optima and miss the global best solution. The positioning error indicates that the random phase values needs to be resolved.

D. Polynomial Regression of Random Phase

Phase ambiguity and device diversity have been overcome in our hyperbola positioning optimization. There is still a challenge remaining to be solved, i.e., random phase. As shown in one of our preliminary empirical studies, the phase values are different even when the target tag is interrogated by the same antenna at the same location. The experiment tells us

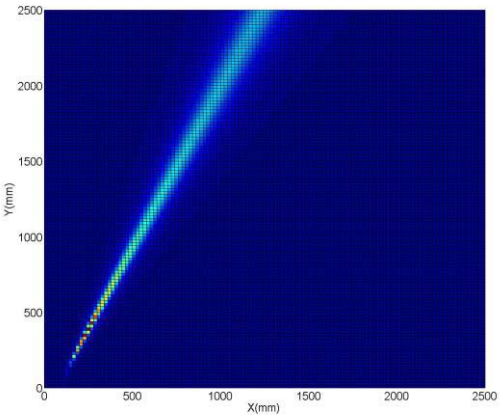

(a)

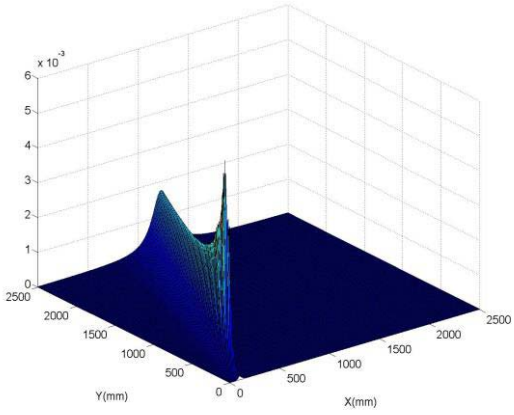

(b)

Fig. 8. Likelihood is the target position of every grid. The pixel value of every grid is assigned as $1/J$. (a) 2-D display of each grid's likelihood. (b) 3-D display of each grid's likelihood.

that complex environment will exert unexpected impact on the phase report, which will lead to measurement error. The correction method is needed to derive the relationship between phase values and distances from the RF noisy environment. Previous works [30], [31] have introduced polynomial regression methods into modeling the relationship between RSSI and distance. In our design, polynomial regression is adopted to remedy the measured phase. The model representation of phase values can be expressed as

$$p_c(t) = c_0 + c_1 t + c_2 t^2 + \cdots c_k t^k \tag{17}$$

where t^k denotes the polynomial variable of timestamp when the tag is interrogated, c_k denotes the parameter that adjusts the model representation to fit the data, and $p_c(t)$ represents the function that maps the variable t to phase value.

The cost function, which is used to evaluate whether the model representation fits the data well, can be defined as

$$J(c) = \frac{1}{2n} \sum_{i=0}^{n-1} (p_c(t_i) - \theta_i)^2 \tag{18}$$

where t_i denotes the times that the target tag is queried for the ith time by the moving antenna and n denotes the times for which the target tag is totally interrogated.

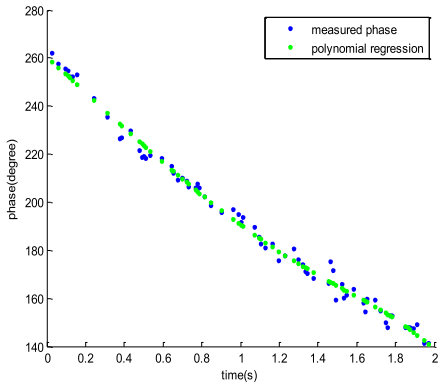

Fig. 9. Polynomial regression of measured phase.

In order to implement polynomial regression, gradient descent method is employed to minimize the cost function. Performing feature scaling can make gradient descent converge much more quickly. The polynomial variables are normalized by subtracting the mean value of each variable first. Then, each feature is divided by their standard deviations. The new variable can be given as

$$t := \frac{t - \mu}{\sigma} \tag{19}$$

where μ is the mean value and σ is the standard deviation.

The major steps of gradient descent are as follows.

1) Initialize parameters, e.g., maximum number of iterations, learning rate α.
2) Loop.
3) Simultaneously update all c_k according to

$$c_k := c_k - \alpha \frac{\partial}{\partial c_k} J(c). \tag{20}$$

4) If exceeding the maximum iteration, exit loop.

Fig. 9 displays the polynomial regression of the measured phase values acquired from antenna motion.

After polynomial regression, we substitute θ_i with $p_c(t_i)$ and the objective function is defined as

$$J = \sum_{i=0}^{n-1} \left(d(X, A_i) - d(X, A_0) - \frac{\lambda}{4\pi} (p_c(t_i) - p_c(t_0) + 2k\pi) \right)^2. \tag{21}$$

Then we implement the PSO method again. The pixel (255, 430) has the highest pixel value and the deviation from the ground truth is about 58.5 mm away. As shown in Fig. 10, the pixel with the highest value is clearly distinct from other pixels.

V. Implementation

We built a prototype based on hyperbola positioning optimization using COTS RFID devices to locate UHF passive target tag. The prototype is run on a 64-bit Dell PC with Inter(R) Core(TM) i7-3770 CPU.

Reader: We adopted a Sirit Infinity 610 reader without any modification of the firmware. The reader is a multiprotocol RFID system that operates in the 860–960 MHz UHF band and the default session of Infinity 610 reader is session 1.

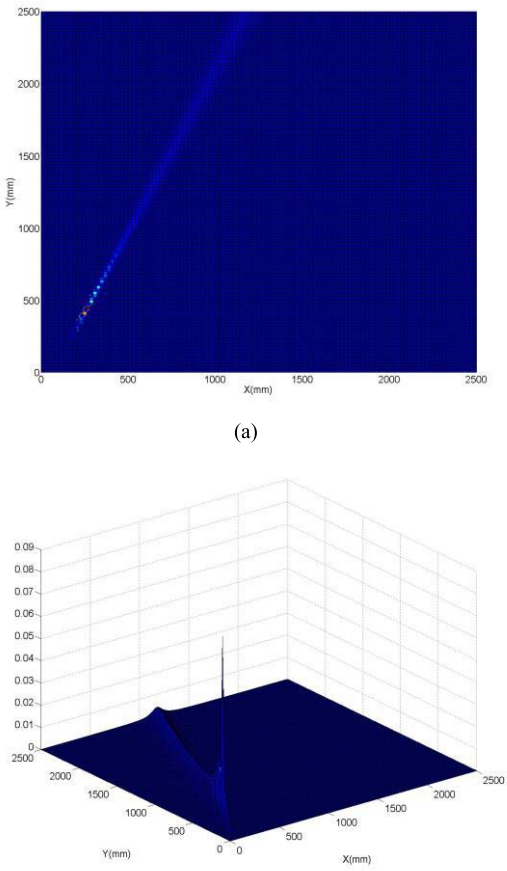

Fig. 10. Likelihood is the target position of every grid after polynomial regression. The pixel value of every grid is assigned as $1/J$. (a) 2-D display of each grid's likelihood. (b) 3-D display of each grid's likelihood.

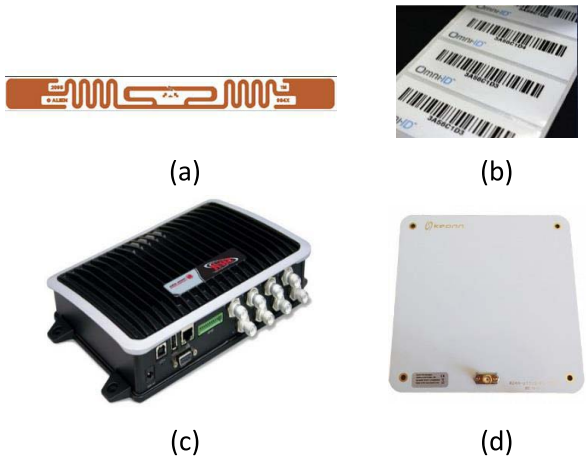

Fig. 11. (a) Alien squiggle tag. (b) Omni-ID tag. (c) Sirit Infinity reader. (d) Keonn p11 antenna.

As shown in Fig. 11, this high-performance reader supports up to eight antennas.

Antenna: We use a circular polarization keonn p11 antenna. The size of the antenna is 137 mm × 137 mm. In order to move the antenna, we put it on a conveyor. The conveyor can move at a constant speed. The antenna's conducted power is set to be 30 dBm.

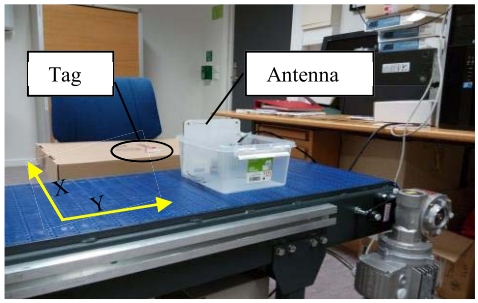

Fig. 12. Deployed experiment with antenna placed on the moving conveyor.

Tag: There are two kinds of tags used in our experiment, as shown in Fig. 11. One is the Omni-ID IQ800P passive RFID tag and another is ALN-9640 Squiggle general purpose tag. Both tags are compatible with EPC Gen2 protocol.

VI. Microbenchmark

We conducted microbenchmark experiments in our laboratory room with size 2.5 m×2.5 m. Fig. 12 shows the laboratory deployment and coordinate system. The performance of hyperbolic positioning optimization is evaluated through comparing with other localization methods and the factors that may affect the accuracy of localization are investigated either.

A. Accuracy Among Different Methods

As aforementioned, there are mainly two types of RFID localization methods, RSSI based and phase based. Therefore, we will compare our method with these two baseline schemes. K nearest neighbor (KNN) is a well-known RSSI-based method and has been widely used in location estimation [7], [10]. BackPos proposed in [32] is selected as comparison because both BackPos and our method rely on the hyperbolic positioning method. The distance from the actual position of the target RFID tag to the calculated position is leveraged as the accuracy metric.

K Nearest Neighbor: KNN employs the RSSI difference between a pair of tags to identify the nearest neighbors and then estimate the target's position based on the KNN algorithm. The RSSI is obtained by deploying four antennas at corners of the room according to the RSSI-based scheme. Although LANDMA*RC* proposed in [7] pinpoints the tag's location using active RFID, the localization method utilized in LANDMARC applies to passive RFID tags in a similar manner.

BackPos: BackPos is a phase-based localization method, which also adopts hyperbolic positioning to locate the RFID tag. However, different from our design, BackPos deploys four stationary antennas in a straight line. Only six hyperbolas can be constructed at the most using this method. In contrast, our method takes advantage of the antenna motion to create the virtual antenna array. Hence, multiple hyperbolas are able to be extracted from the antenna motion.

1) Tag Orientation: First, we evaluate the impact of tag orientation on accuracy among different methods. Omni-ID tag is employed in this experiment. We place the target tag at a fixed location and adjust its orientation from 0° to 315°. In this experiment, the tag is located at x = 0.9 m and

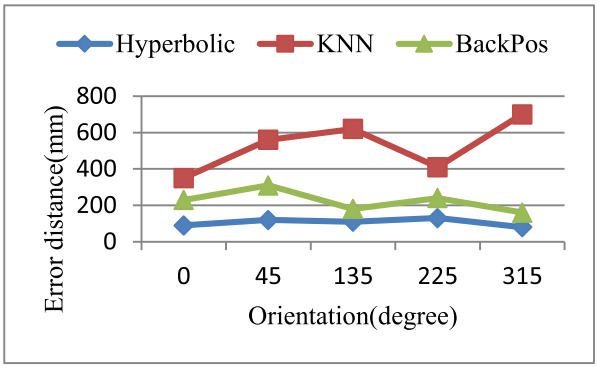

Fig. 13. Impact of tag orientation on positioning accuracy.

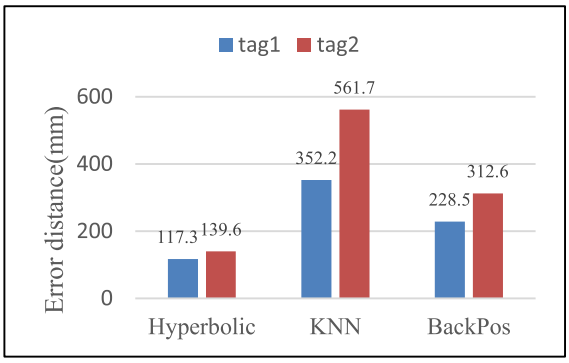

Fig. 14. Impact of tag diversity on positioning accuracy.

y = 1.5 m. The antenna is moving along $x = [0.35 \ldots 0.95]$ m and $y = 0$. As illustrated in Fig. 3, the tag orientation is the angle between the tag's antenna and the reader antenna's polarization direction. The accuracy of the three methods at different tag orientations is shown in Fig. 13.

From Fig. 13, we can see that the accuracy almost remains unchanged for hyperbolic positioning. Tag orientation has impact on the accuracy of BackPos method, but not too much. However, the accuracy of KNN is severely affected by the tag orientation. Actually, this result is not unexpected, as KNN relies on the RSSI value to locate the object. When the angle between reader antenna and tag antenna varies, the RSSI value will change dramatically. Therefore, phase value is more reliable to locate object compared with RSSI value.

2) Tag Diversity: Tag diversity is another factor affecting the accuracy, which cannot be neglected in positioning. We conduct an experiment to measure the impact of tag diversity on different methods. Two kinds of tags are employed in our experiment. Tag1 is Omni-ID IQ800P and tag 2 is alien squiggle general-purpose tag. We place the target tag at ten different locations with a fixed orientation as shown in Fig. 15. The comparison among the three methods is shown in Fig. 14. In our design, the tag diversity is eliminated by phase difference. Therefore, the accuracy of hyperbolic positioning varies a little on different tags. Similarly, BackPos deals with tag diversity in the same way as our methods. Hence, it is less affected by tag diversity. On the contrary, tag diversity is not taken into consideration in the RSSI-based algorithm. Consequently, it is not surprising for LANDMARC to have different accuracies on different tags.

3) Cumulative Distribution Function: We attach an Omni-ID tag to the target object and place the Omni-ID tag with random orientation at ten different positons as shown in Fig. 15. The antenna is moving along $x = [0.35 \ldots 0.95]$ m and $y = 0$. The experiment is repeated over ten times. Fig. 16 displays the cumulative distribution function (CDF) of error distance based on different localization algorithms.

The median error of KNN is 497.06 mm, and the 90th percentile is 662.2309 mm. This accuracy is consistent with the result acquired in [6].

BackPos achieves median error distance of 253.89 mm and the 90th percentile is 375.2772 mm, which is a 50% reduction compared with the RSSI-based method. Previous works [32], [33] have also reported that phase-based localization is better than the RSSI-based method.

Our design has a median error distance 122.25 mm and 90th percentile 197.96 mm, outperforming RSSI-based and phase-based by 5× and 2×, respectively. Several reasons underlie the significant improvement. First, phase measurement is indeed a reliable indicator for positioning and is a more robust positioning metric regardless of tag orientation and tag diversity. As shown in Figs. 13 and 14, phase-based methods have less error distance compared to RSSI-based methods. Second, hyperbolic positioning optimization overcomes the device diversity successfully, which severely affect the accuracy of positioning. Third, antenna motion could help reader query RFID tag from multiple different directions, which can effectively weaken the impact of multipath.

B. Accuracy With and Without Polynomial Regression

Next, we conduct experiment to compare the accuracy between hyperbolic positioning optimization algorithm with and without polynomial regression. Their error distances are shown in Fig. 17. The algorithm without polynomial regression has a median error distance of 166.7 mm and 90th percentile is 260.6 mm, whereas the algorithm with polynomial regression improves the accuracy to median error distance of 122.2 mm and its 90th percentile is 197.9 mm. As illustrated in Fig. 16, random phase indeed leads positioning error, and polynomial regression can reduce its effect successfully though the accuracy is not improved too much. This result demonstrates that the influence of random phase could be statistically suppressed to some extent through a combination of multiple hyperbolas.

C. Evaluation of RFID Parameters on Performance

1) Read Time: The read time signifies the interval between two consecutive phase measurements. In order to evaluate the impact of read time on the performance, we set the read time to be 25, 50, and 100 ms, respectively. For a tag located at $x = 0.9$ m and $y = 1.5$ m, the antenna is moving along $x = [0.35 \ldots 0.95]$ m and $y = 0$. It can be seen from Table I that with the increase of read time, the accuracy of our system decreases instead. When the read time is 100 ms, the number of phase measurement is 30. The insufficient phase measurements are not able to ensure the high accuracy.

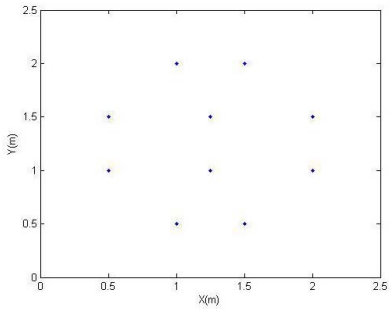

Fig. 15. Distribution of test points.

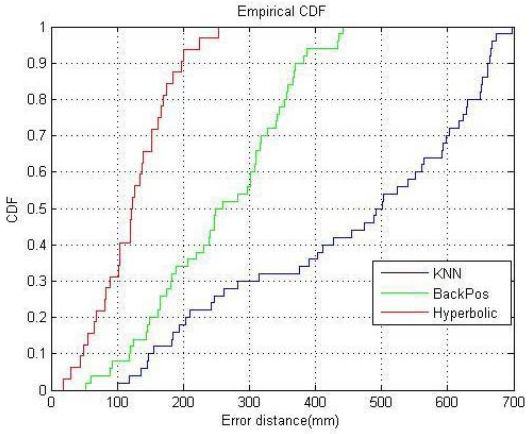

Fig. 16. CDF of localization error among KNN, BackPos, and hyperbolic positioning optimization.

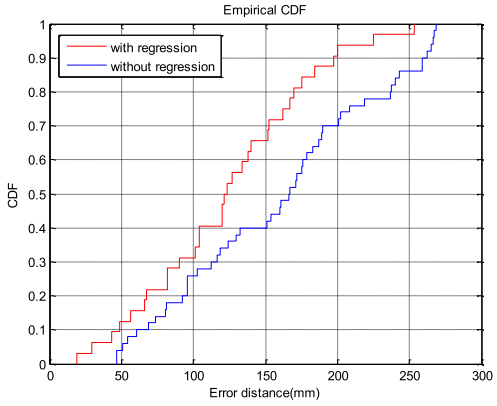

Fig. 17. CDF of localization error between with and without polynomial regression.

2) Frequency Channel: In Europe, the UHF RFID hops between four channels, i.e., 865700, 866300, 866900, and 867500 KHz. Given a specific read time, we investigate the impact of RFID frequency on the performance of our system. The results in Table I show that the influence of frequency is much less than the read time. The positioning accuracy of our system does not have much relationship with the frequency.

3) Impact of Distance: The tag locations in Fig.15 can be grouped into four sets, 0.5 to 2 m meters away from the moving antenna. The error distance of each group is depicted in Fig. 18. As shown in the figure, the performance of our design has no clear correlation with the distance between the

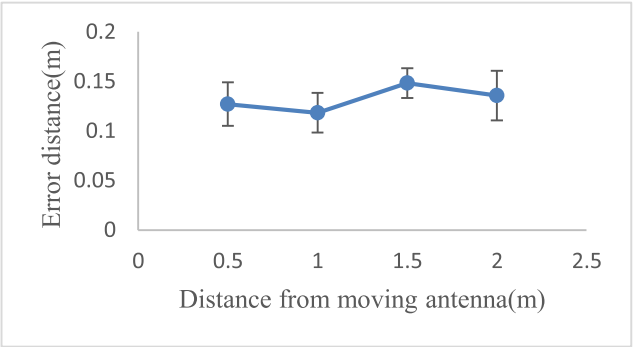

Fig. 18. Impact of distance from the antenna.

TABLE I
IMPACT OF RFID PARAMETERS

Read Time(ms)	Frequency(KHz)			
	865700	866300	866900	867500
	Positioning accuracy(m)			
25	0.1271	0.1315	0.1183	0.1357
50	0.1483	0.1532	0.1360	0.1400
100	0.1745	0.1792	0.1747	0.1825

tag and the moving antenna. The mean error distance of all the groups achieves 0.1323 m. This result agrees with the outcome reported for AOA-based method [32].

VII. CONCLUSION

In this paper, we present hyperbolic positioning optimization algorithm for the positioning of UHF passive RFID tags. Aimed to reduce the cost of RFID positioning system and make it easy to implement, we only use COTS devices without any modification of the firmware. In addition, reference tags are not needed in our design. The key innovations of our design are to construct multiple hyperbola curves through motion antenna and introduce the PSO method into positioning to enhance computational ability. Since we emulate antenna array via moving antenna, the space between two virtual antennas is much less than half the wavelength. Therefore, phase ambiguity can be avoided in this way. Another benefit from motion antenna is device diversity can be eliminated easily. In order to tackle random phase owing to the RF noisy environment, polynomial regression is adopted to remedy the measured phase values and could improve the positioning accuracy further. A variety of experiments is conducted; the results demonstrate that our method is independent of tag diversity and tag orientation. Moreover, the accuracy could achieve centimeter level. Future research will focus on the following aspects. First, the phase measurements collected from the moving reader is processed offline. A real-time system is needed to be developed in the future. Second, our approach is mainly presented in a 2-D scenario. Theoretically, it can be easily extended into 3-D space, but the computation complexity will increase correspondingly. The computation cost of PSO applied in 3-D scenario needs to be investigated further.

REFERENCES

[1] Impinj. (2015). *How Do RFID Systems Work?* [Online]. Available: http:/www.impinj.com/resources/about-rfid/how-do-rfid-systems-work/

[2] H.-D. Chen, C.-H. Tsai, C.-Y.-D. Sim, and C.-Y. Kuo, "Circularly polarized loop tag antenna for long reading range RFID applications," *IEEE Antennas Wireless Propag. Lett.*, vol. 12, pp. 1460–1463, 2013.

[3] J. Wang, F. Adib, R. Knepper, D. Katabi, and D. Rus, "RF-compass: Robot object manipulation using RFIDs," in *Proc. 19th Annu. Int. Conf. Mobile Comput. Netw. (MobiCom)*, 2013, pp. 3–14.

[4] A. A. N. Shirehjini, A. Yassine, and S. Shirmohammadi, "Equipment location in hospitals using RFID-based positioning system," *IEEE Trans. Inf. Technol. Biomed.*, vol. 16, no. 6, pp. 1058–1069, Nov. 2012.

[5] D. Laqua *et al.*, "Wireless equipment localization for medical environments," in *Proc. World Congr. Med. Phys. Biomed. Eng.*, 2015, pp. 1453–1456.

[6] L. Yang, Y. Chen, X.-Y. Li, C. Xiao, M. Li, and Y. Liu, "Tagoram: Real-time tracking of mobile RFID tags to high precision using COTS devices," in *Proc. 20th Annu. Int. Conf. Mobile Comput. Netw. (MobiCom)*, 2014, pp. 237–248.

[7] L. M. Ni, Y. Liu, Y. C. Lau, and A. P. Patil, "LANDMARC: Indoor location sensing using active RFID," *Wireless Netw.*, vol. 10, no. 6, pp. 701–710, 2004.

[8] Y. Zhao, Y. Liu, and L. M. Ni, "VIRE: Active RFID-based localization using virtual reference elimination," in *Proc. Int. Conf. Parallel Process. (ICPP)*, Sep. 2007, p. 56.

[9] M. Hasani, J. Talvitie, L. Sydänheimo, E. S. Lohan, and L. Ukkonen, "Hybrid WLAN-RFID indoor localization solution utilizing textile tag," *IEEE Antennas Wireless Propag. Lett.*, vol. 14, pp. 1358–1361, 2015.

[10] X. Luo, W. J. O'Brien, and C. L. Julien, "Comparative evaluation of received signal-strength index (RSSI) based indoor localization techniques for construction jobsites," *Adv. Eng. Inform.*, vol. 25, no. 2, pp. 355–363, 2011.

[11] F. Martinelli, "A robot localization system combining RSSI and phase shift in UHF-RFID signals," *IEEE Trans. Control Syst. Technol.*, vol. 23, no. 5, pp. 1782–1796, Sep. 2015.

[12] A. Buffi, P. Nepa, and F. Lombardini, "A phase-based technique for localization of UHF-RFID tags moving on a conveyor belt: Performance analysis and test-case measurements," *IEEE Sensors J.*, vol. 15, no. 1, pp. 387–396, Jan. 2015.

[13] S. Azzouzi, M. Cremer, U. Dettmar, R. Kronberger, and T. Knie, "New measurement results for the localization of UHF RFID transponders using an angle of arrival (AoA) approach," in *Proc. IEEE Int. Conf. (RFID)*, Apr. 2011, pp. 91–97.

[14] H.-C. Chen, T.-H. Lin, H. T. Kung, C.-K. Lin, and Y. Gwon, "Determining RF angle of arrival using COTS antenna arrays: A field evaluation," in *Proc. MILCOM*, Oct. 2012, pp. 1–6.

[15] J. Xiong and K. Jamieson, "ArrayTrack: A fine-grained indoor location system," in *Proc. 10th USENIX NSDI*, 2013, pp. 71–84.

[16] C. Zhou and J. D. Griffin, "Accurate phase-based ranging measurements for backscatter RFID tags," *IEEE Antennas Wireless Propag. Lett.*, vol. 11, pp. 152–155, 2012.

[17] C. Hekimian-Williams, B. Grant, X. Liu, Z. Zhang, and P. Kumar, "Accurate localization of RFID tags using phase difference," in *Proc. IEEE Int. Conf. (RFID)*, Apr. 2010, pp. 89–96.

[18] J. Huiting, H. Flisijn, A. B. J. Kokkeler, and G. J. M. Smit, "Exploiting phase measurements of EPC Gen2 RFID tags," in *Proc. IEEE Int. Conf. RFID-Technol. Appl. (RFID-TA)*, Sep. 2013, pp. 1–6.

[19] J. Wang and D. Katabi, "Dude, where's my card?: RFID positioning that works with multipath and non-line of sight," *ACM SIGCOMM. Comput. Commun. Rev.*, vol. 43, no. 4, pp. 51–62, 2013.

[20] R. Miesen, F. Kirsch, and M. Vossiek, "UHF RFID localization based on synthetic apertures," *IEEE Trans. Autom. Sci. Eng.*, vol. 10, no. 3, pp. 807–815, Jul. 2013.

[21] A. Parr, R. Miesen, and M. Vossiek, "Inverse SAR approach for localization of moving RFID tags," in *Proc. IEEE Int. Conf. (RFID)*, Apr. 2013, pp. 104–109.

[22] M.-C. Hua, G.-C. Peng, Y.-J. Lai, and H.-C. Liu, "Angle of arrival estimation for passive UHF RFID tag backscatter signal," in *Proc. IEEE Int. Conf. (iThings/CPSCom)*, Aug. 2013, pp. 1865–1869.

[23] H. Zou, H. Wang, L. Xie, and Q.-S. Jia, "An RFID indoor positioning system by using weighted path loss and extreme learning machine," in *Proc. IEEE 1st. Int. Conf. Cyber-Phys. Syst., Netw., Appl. (CPSNA)*, Aug. 2013, pp. 66–71.

[24] L. Shangguan, Z. Li, Z. Yang, M. Li, and Y. Liu, "Otrack: Order tracking for luggage in mobile RFID systems," in *Proc. IEEE INFOCOM*, Apr. 2013, pp. 3066–3074.

[25] S. Särkkä, V. V. Viikari, M. Huusko, and K. Jaakkola, "Phase-based UHF RFID tracking with nonlinear Kalman filtering and smoothing," *IEEE Sensors J.*, vol. 12, no. 5, pp. 904–910, May 2012.

[26] R. Kronberger, T. Knie, R. Leonardi, U. Dettmar, M. Cremer, and S. Azzouzi, "UHF RFID localization system based on a phased array antenna," in *Proc. IEEE Int. Symp. Antennas Propag. (APSURSI)*, Jul. 2011, pp. 525–528.

[27] Sirit, "Application note for tag phase reporting technology," Sirit Technol., Toronto, ON, Canada, Appl. Note version 1.1, 2009.

[28] D. P. Rini, S. M. Shamsuddin, and S. S. Yuhaniz, "Particle swarm optimization: Technique, system and challenges," *Int. J. Comput. Appl.*, vol. 14, no. 1, pp. 19–26, 2011.

[29] Y. J. Gong, M. Shen, J. Zhang, O. Kaynak, W. N. Chen, and Z. H. Zhan, "Optimizing RFID network planning by using a particle swarm optimization algorithm with redundant reader elimination," *IEEE Trans. Ind. Informat.*, vol. 8, no. 4, pp. 900–912, Nov. 2012.

[30] Z. Cao, Z. Yuan, and S. Zhang, "Experimental exploration of RSSI model for the vehicle intelligent position system," *J. Ind. Eng. Manage.*, vol. 8, no. 1, pp. 51–71, 2015.

[31] T. Sullivan, J. Jo, and M. Lennon, "A usability study for signal strength based localisation," in *Robot Intelligence Technology and Applications 3*. Cham, Switzerland: Springer, 2015, pp. 35–44.

[32] T. Liu, L. Yang, Q. Lin, Y. Guo, and Y. Liu, "Anchor-free backscatter positioning for RFID tags with high accuracy," in *Proc. IEEE INFOCOM*, Apr. 2014, pp. 379–387.

[33] P. V. Nikitin, R. Martinez, S. Ramamurthy, H. Leland, G. Spiess, and K. V. S. Rao, "Phase based spatial identification of UHF RFID tags," in *Proc. IEEE Int. Conf. (RFID)*, Apr. 2010, pp. 102–109.

Haishu Ma received the B.S. degree in mechanical engineering from the Henan Institute of Engineering, Zhengzhou, China, in 2011, and the M.S. degree in mechanical automation from Shanghai University, Shanghai, China, in 2014. He is currently pursuing the Ph.D. degree with the Department of Production and Quality Engineering, Norwegian University of Science and Technology, Trondheim, Norway.

He is involved in integrating computation intelligence with RFID-based indoor positioning algorithm. His current research interests focus on indoor localization and machine learning.

Yi Wang received the Ph.D. degree from the Manufacturing Engineering Center, Cardiff University, Cardiff, U.K., in 2008.

He is a Lecturer in fashion logistics with the School of Materials, University of Manchester, Manchester, U.K. He has published 26 technical peer-reviewed papers in international journals and conferences. He has co-authored two books: *Operations Management for Business* and *Data Mining for Zero-Defect Manufacturing*. He has special research interests in supply chain management, RFID, logistics, operation management, culture management, information systems, game theory, data analysis, semantics and ontology analysis, and neuromarketing.

Kesheng Wang received the Ph.D. degree in production engineering from the Norwegian University of Science and Technology (NTNU), Trondheim, Norway, in 1988.

He was an elected member of the Norwegian Academy of Technological Sciences, Trondheim, in 2006. Since 1993, he has been a Professor at the Department of Production and Quality Engineering, NTNU. He is currently the Director of the Knowledge Discovery Laboratory, NTNU. He is also an active researcher and serves as a Technical Adviser at SINTEF, Trondheim. He has published 19 books, 10 book chapters, and over 240 technical peer-reviewed papers in international journals and conferences. His current areas of interest are intelligent manufacturing systems, applied computational intelligence, data mining and knowledge discovery, swarm intelligence, condition-based monitoring and structured light systems for 3-D measurements and RFID, and predictive maintenance and industry 4.0.

Zongzheng Ma received the B.S. and M.S. degrees in mechanical engineering from Shandong Jianzhu University, Jinan, China, in 2004 and 2007, respectively, and the Ph.D. degree in thermal engineering from Shandong University, Jinan, in 2010.

From 2012 to 2014, he was a Research Assistant with the Mechanical Engineering Department, Henan Institute of Engineering, Zhengzhou, China. He joined the Knowledge Discovery Laboratory, Norwegian University of Science and Technology, as a Visiting Researcher in 2016. Since 2014, he has been an Assistant Professor with the Mechanical Engineering Department, Henan University of Engineering, Zhengzhou. He has authored four books, more than 30 articles, and more than 10 inventions.

Prof. Ma was a recipient of Key Members of the Outstanding Young Teacher of Henan Province in 2014 and the Best Science Paper Award of Henan Province in 2015.